LASER INTERFEROMETER GRAVITATIONAL WAVE OBSERVATORY
- LIGO -
CALIFORNIA INSTITUTE OF TECHNOLOGY
MASSACHUSETTS INSTITUTE OF TECHNOLOGY

Technical Note	**LIGO-T11XXXXX–vX**	2017/06/02

Squeezing Quantum Noise with Waveguides
Interim Report for SURF 2017

Dhruva Ganapathy

California Institute of Technology
LIGO Project, MS 18-34
Pasadena, CA 91125
Phone (626) 395-2129
Fax (626) 304-9834
E-mail: info@ligo.caltech.edu

Massachusetts Institute of Technology
LIGO Project, Room NW22-295
Cambridge, MA 02139
Phone (617) 253-4824
Fax (617) 253-7014
E-mail: info@ligo.mit.edu

LIGO Hanford Observatory
Route 10, Mile Marker 2
Richland, WA 99352
Phone (509) 372-8106
Fax (509) 372-8137
E-mail: info@ligo.caltech.edu

LIGO Livingston Observatory
19100 LIGO Lane
Livingston, LA 70754
Phone (225) 686-3100
Fax (225) 686-7189
E-mail: info@ligo.caltech.edu

http://www.ligo.caltech.edu/

1 Introduction

1.1 LIGO

The LIGO gravitational wave detectors are specialized versions of a Michelson interferometer with 4 km long arms with Fabry Perot cavities. Its peak design sensitivity is 3.5×10^{-24} in the 100 Hz band[1] , When it reaches design sensitivity it will be quantum noise limited over much of the detection band[2]. The Advanced LIGO (aLIGO) detectors came online in September 2015, after a major upgrade targeting a factor of 10 sensitivity improvement over initial detectors. The two test masses are placed 4 km apart and form an optical resonator with a gain of 300. The suspension system provides high isolation above the resonance frequencies which range from 0.4 to 13 Hz.

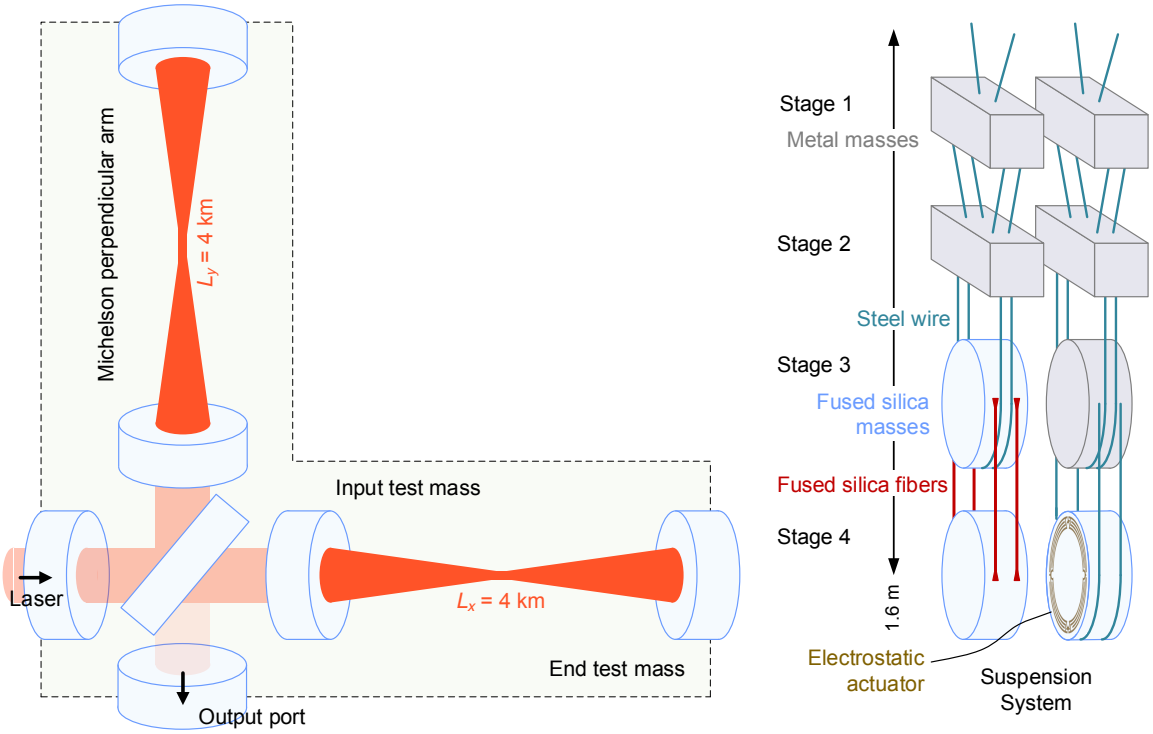

Figure 1: aLIGO

1.2 Squeezed Light

In an upgrade to aLIGO [3], work is underway to install a parametric oscillator squeezed vacuum light source to reduce quantum shot noise which limits the sensitivity of gravitational wave detector. This noise arises due to vacuum fluctuations which occur due to Heisenbergs uncertainty principle which states that $\Delta X \Delta Y > 1$ where X and Y are uncertainty in the quadratures associated with the photon field and are given by the expressions :

$$X = (a + a^\dagger)$$

$$Y = -i(a - a^\dagger)$$

Where a and $a\dagger$ are bosonic annihilation and creation operators respectively.

Vacuum is the ground state of a photon field and it is a coherent state. Coherent states are minimum uncertainty states where $\Delta X = \Delta Y = 1$. These uncertainties give rise to vacuum fluctuations which enter the unused port of the interferometer of the gravitational wave detector. The noise arising from these uncertainties can be understood by Figure 2.

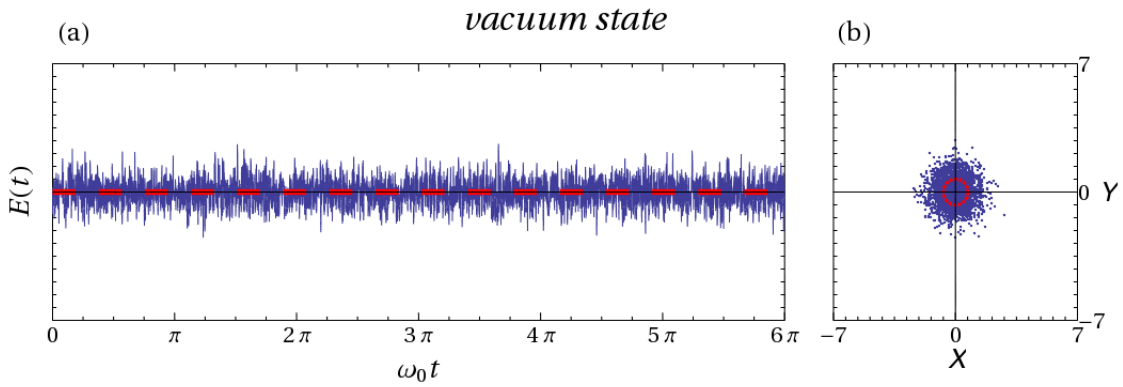

Figure 2: Electric Field in Coherent Vacuum

Squeezed states are also minimum uncertainty states. Here, the noise in one quadrature is greater than that in the other. Replacing the vacuum fluctuations with squeezed states in GW interferometers can reduce the quantum noise measured by the detector.

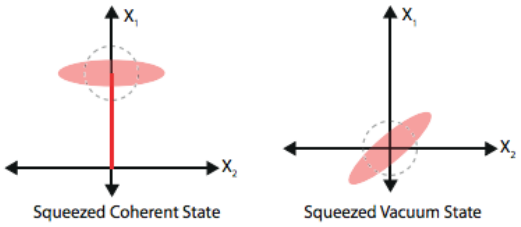

Figure 3: Quadrature Diagrams for Squeezed Light

Squeezing has already been implemented twice in working GW detectors [4],[5] and is a proven technology for enhancing signal to shot noise sensitive by 3.5 dB and 2.1 dB for the GEO600 and Enhanced LIGO detectors respectively. Squeezing injection is planned as a permanent feature in the next round of intermediate upgrades. More details about squeezed light can be found in [6].

2 Project

2.1 Objective

This project will investigate the spatial mode profiles emitted from a wave-guide type non-linear squeezer devices, examine the optimum index profile, pumping field shape and out

coupling scheme for generating high quantum efficiency modes for use in free space, and investigate how imperfections in the mode shapes affect the level of squeezing improvement ultimately achievable in a GW detector.

2.2 Approach

2.2.1 Setup

The project setup is shown in Figure 4. The Innolight Diabolo laser is a source of 532 nm and 1064 nm photons for the experiment. It consists of a 1.5 W Nd:YAG NPRO laser (pumped with two banks of diode lasers) with most of this light tapped off to an SHG unit for conversion to 532 nm. The green 532nm photons undergo Spontaneous Parametric Down-Conversion in a compact non-linear waveguide. Single mode squeezing is obtained when the SPDC is degenerate, i.e, the produced photons are indistinguishable.

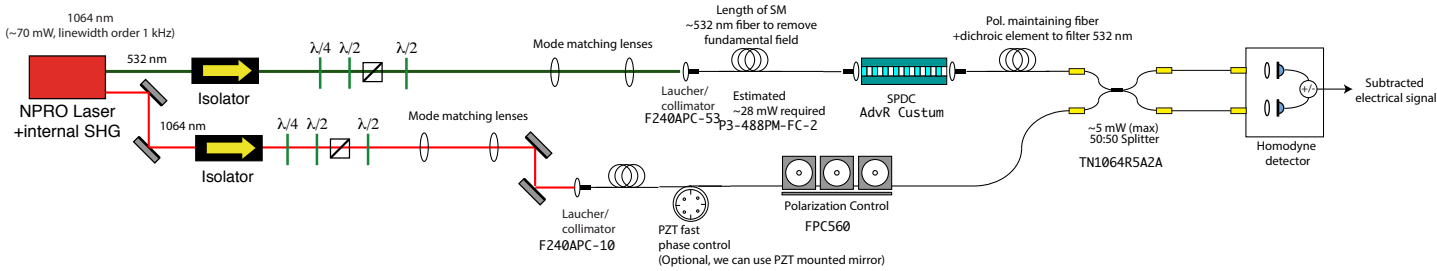

Figure 4: Proposed Setup for Waveguide Experiment

2.2.2 Beam Profiling

The properties of the Gaussian beam depend only on the size of the waist w_0 and the wavelength λ. It is therefore possible to fully characterize a Gaussian beam by determining the size and location of the beam waist. To determine these quantities, we make a series of 'knife edge' measurements to determine the spot size on different axial locations.

We record the total power in the beam as a knife edge is translated through the beam using a calibrated translation stage. This gives us the integral of the power from $-\infty$ to the knife edge location.

In one direction this power is given by

$$P(y) = \frac{P_{total}}{2}(1 - (\frac{\sqrt{2}y}{w_y}))$$

Fitting the obtained power to the above function gives us the spot size at the location of profiling

The obtained spot sizes are fit to the function

$$w(z) = w_0\sqrt{1 + (\frac{z - z_0}{z_r})^2}$$

where $z_r = \dfrac{\pi w_0^2}{\lambda}$

in order to find the beam waist size and location

2.2.3 Mode Matching and Beam Propagation

One part of this project would involve modelling mode-matching between the wave-guide and the optical cavity of the resonator. For the optical waveguide, we will be considering a rectangular core waveguide with a step index.

To find the mode shapes of this waveguide, we can assume a separable solution of the scalar wave equation in rectangular coordinates.

$$\frac{\partial^2\psi}{\partial x^2} + \frac{\partial^2\psi}{\partial y^2} + [k_o^2 n^2(x, y) - \beta^2] = 0 \tag{1}$$

where β is the propagation constant and k_o is the free space wave number.

The solution obtained for this equation is given by

$$\psi = \begin{cases} A\cos\mu_1\xi\cos\mu_2\eta & \text{if} |\xi| \le 1, |\eta| \le 1 \\ \dfrac{A\cos\mu_2}{\exp[-(V_2^2 - \mu_2^2)]^{\frac{1}{2}}}\cos\mu_1\xi\exp[-(V_2^2 - \mu_2^2)\eta]^{\frac{1}{2}} & \text{if } |\xi| \ge 1, |\eta| \le 1 \\ \dfrac{A\cos\mu_1}{\exp[-(V_1^2 - \mu_1^2)]^{\frac{1}{2}}}\cos\mu_2\eta\exp[-(V_1^2 - \mu_1^2)\xi]^{\frac{1}{2}} & \text{if } |\xi| \le 1, |\eta| \ge 1 \\ \dfrac{A\cos\mu_1}{\exp[-(V_1^2 - \mu_1^2)]^{\frac{1}{2}}\exp[-(V_2^2 - \mu_2^2)\eta]^{\frac{1}{2}}}\exp[-(V_2^2 - \mu_2^2)\eta]^{\frac{1}{2}}\exp[-(V_1^2 - \mu_1^2)\xi]^{\frac{1}{2}} & \text{if } |\xi| \ge 1, |\eta| \ge 1 \end{cases} \tag{2}$$

where

$$\xi = (2x/a), \quad \eta = (2y/b), \quad V_1 = k_o\frac{a}{2}(n_1^2 - n_2^2)^{\frac{1}{2}}, \quad V_2 = k_o\frac{b}{2}(n_1^2 - n_2^2)^{\frac{1}{2}}$$

$$\mu_1 = \frac{a}{2}(k_o^2 n_1^2 - \beta^2)^{\frac{1}{2}}, \quad \mu_2 = \frac{b}{2}(k_o^2 n_1^2 - \beta^2)^{\frac{1}{2}}$$

A detailed solution of this equation is described in [7]. The effect of imperfections in the step index can be modelled by methods such as perturbation and scalar variational methods.

The normal modes supported by the optical cavity, or any complex paraxial optical system, are higher order Gaussian or Hermite-Gaussian modes. These modes are given by

$$\tilde{u}_n = \tilde{\alpha}_n\tilde{v}^n H_n(\frac{\sqrt{2}x}{\tilde{v}})\exp(-\frac{r^2}{w(z)^2})\exp(-i\frac{kr^2}{2R(z)})\exp(-i(kz - \psi(z)))$$

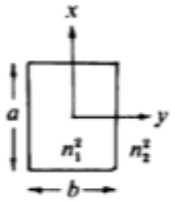

Figure 5: Rectangular Core Waveguide

where H_n is the n^{th} order Hermite polynomial, and $\psi(z)$ is the Gouy Phase of the beam

2.3 Beam Propagation

2.3.1 ABCD Propagation

When a Gaussian beam propagates in free space, it remains Gaussian, while its spot size and radius of curvature vary according to the wave equation. Now the beam at a point can be characterised by the following quantity.

$$q = z + iz_r$$

where z_r is the Rayleigh range of the beam, and z is the distance of the point from the waist.

The inverse of q contains a information about the spot size and radius of curvature of the beam. Substituting $w(z)$ and $R(z)$, we get

$$\frac{1}{q} = \frac{1}{R(z)} - \frac{i\lambda}{\pi w^2(z)}$$

If we specify the initial value of q, then we can use the ABCD propagation matrices for determining the final value of q[8].

$$q_2 = \frac{Aq_1 + B}{Cq_1 + D}$$

The matrices that we use in this project are -

$$\begin{pmatrix} A & B \\ C & D \end{pmatrix} = \begin{pmatrix} 1 & d \\ 0 & 1 \end{pmatrix}$$

for free space propagation through distance d and

$$\begin{pmatrix} A & B \\ C & D \end{pmatrix} = \begin{pmatrix} 1 & 0 \\ -\frac{1}{f} & 1 \end{pmatrix}$$

for propagation through lens with focal length f.

2.3.2 FFT Propagation

While ABCD propagation is a convinient method and can be used as a reference for other propagation methods, it is only applicable to the mode shapes of Gaussian beams. The mode outside the waveguide will not be a Gaussian and we will need other methods to find its mode shape after propagation in free space. One such method that we have implemented is FFT propagation of the beam[9].

According to the Huygens integral,

$$E(x,y,z) = \frac{i}{\Delta z \lambda} \iint E_0(x,y,z_0) K(x-u, y-v, \Delta z) du dv$$

which can be seen as a convolution of the source field E_0 at z_0 and the paraxial diffraction kernel.

In the fourier space, this is just the product of the Fourier Transform of the field and the FT of the diffraction kernel which is given by

$$\tilde{K}(p,q,\Delta z) = \exp\left(-i\frac{\Delta z(p^2+q^2)}{2k}\right)$$

.

The final mode can be found out by taking an inverse fourier transform of the product. In our code we have used the fft2, and ifft2 functions of MATLAB to implement this routine.

2.3.3 Detecting Squeezed States

Balanced homodyne is an interference setup that is used for quadrature measurements. The field that is to be measured is overlapped with a local oscillator on a symmetric beam splitter, whose outputs impinge of two photodiodes, whose photocurrents are electronically subtracted. The phase of the local oscillator beam is controlled via a piezzo-electric transducer. The subtracted photocurrent is analysed using time domain and frequency domain approaches as described in [6].

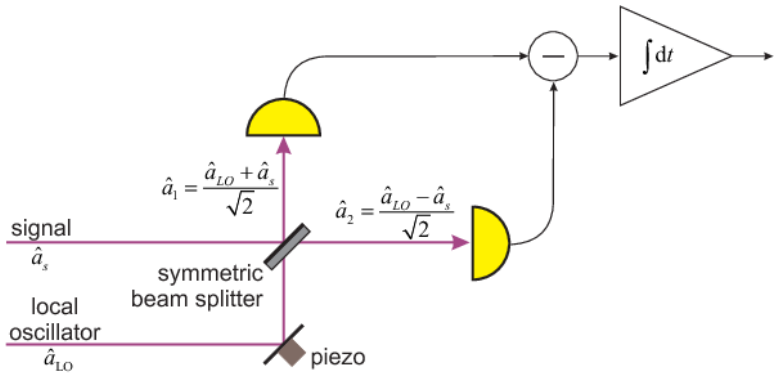

Figure 6: Balanced Homodyning Scheme

In order to properly detect squeezed states, we also need to take into account the noise that affects the homodyning process. The source of this noise includes electronic noise such as flicker in resistors and dark noise of photodiode, and optical noise due to scattering loss, photodiode inhomogeneity and parasitic interferences. These sources and methods to reduce them have been described in [10].

2.4 Progress

2.4.1 Beam Profiling

Following are a few results from profiling a He-Ne laser, in preparation for profiling the Diabolo laser.

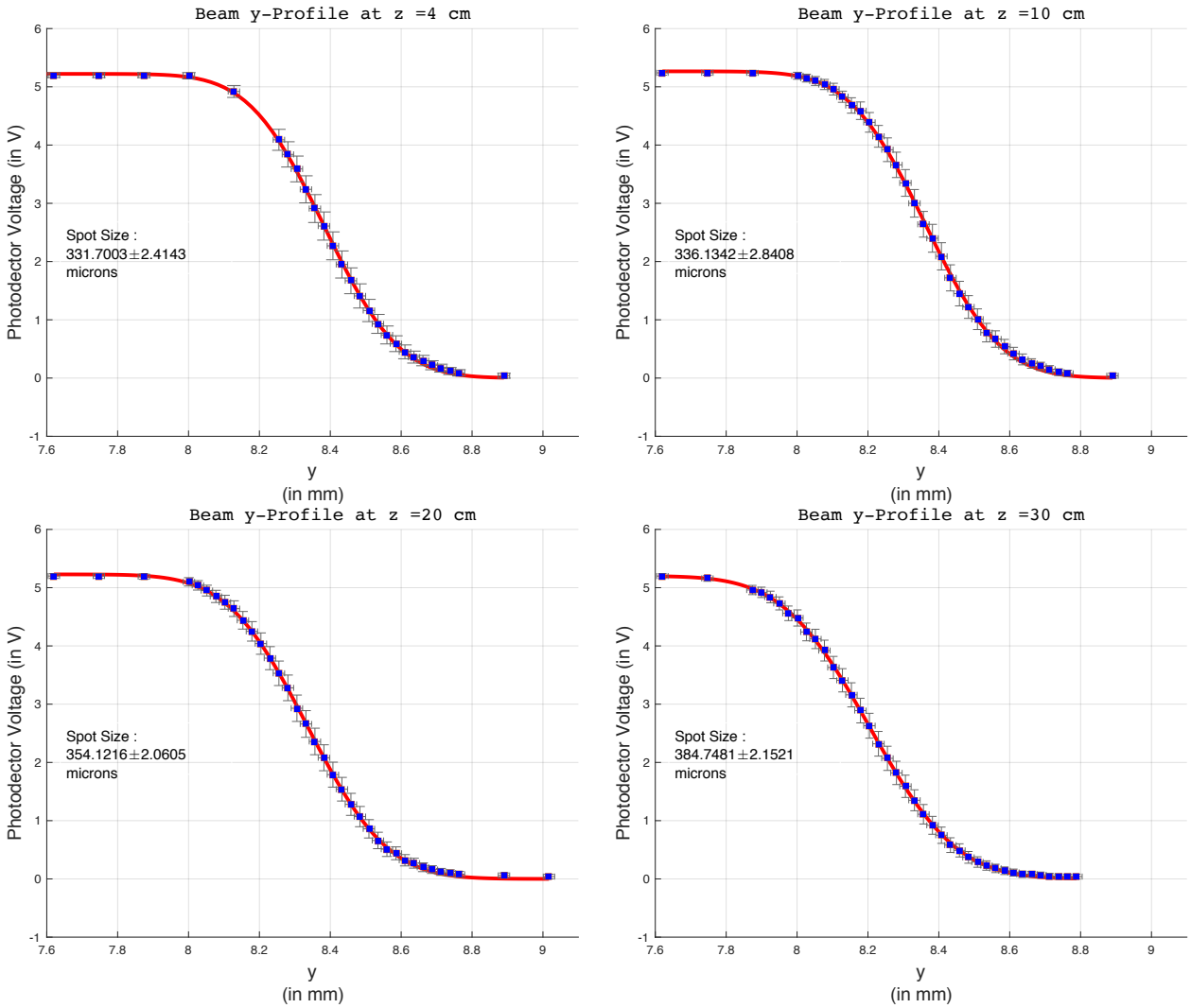

Figure 7: Beam Profiling Results

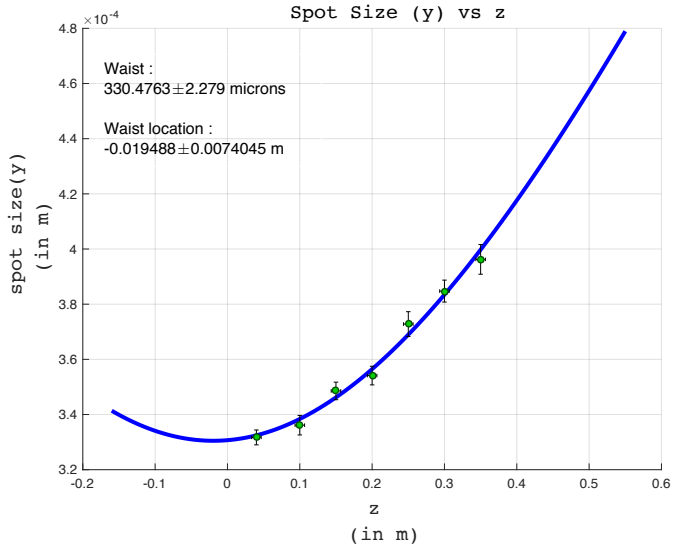

Figure 8: Beam Waist Size and Location

We see that the obtained spot size values fit within σ to the function described in Section 2.2.2.

2.4.2 ABCD Propagation

In this example below, we propagate a beam which has an initial ROC of ∞ and initial spot size of 200 μm. We pass it through a 6cm converging lens at z=10cm.

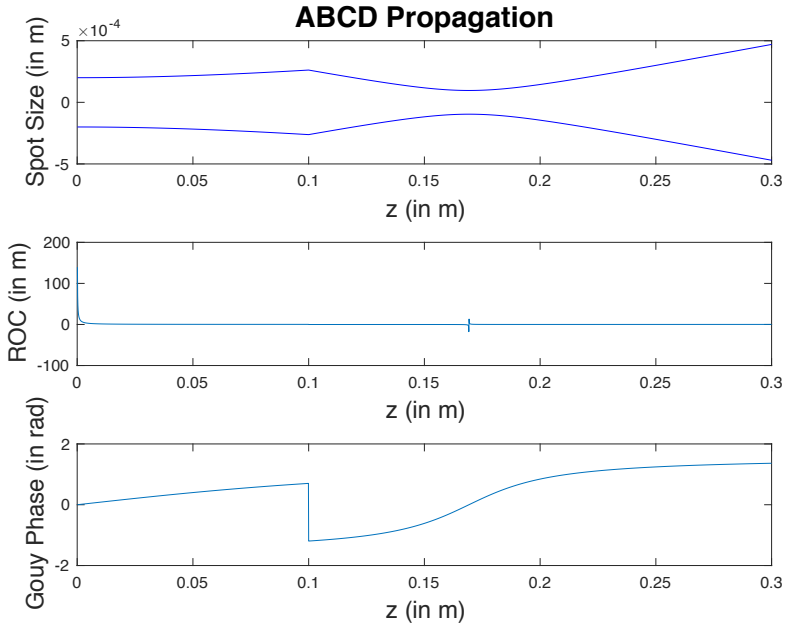

Figure 9: $w_0 = 200\mu$m, $\lambda = 1064$nm with a lens(f = 6cm) placed at z = 10cm

At z = 10cm, the spot size is 262μm and at z = 16.9, at the next beam waist, the spot size of the beam is 96.26 μm

We can also, on magnifying the ROC plot, that see that the radius of curvature changes sign after the lens as it goes from diverging to converging.This blows up at the 16.9cm, where it goes to ∞ (waist).

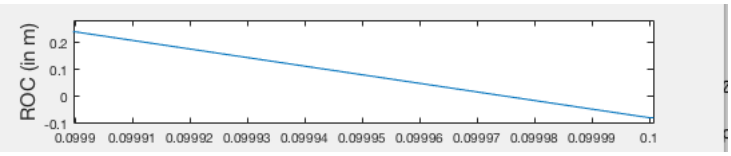

Figure 10: Magnified plot of ROC

2.4.3 FFT Propagation

Using the same conditions and parameters of the beam in Figure 9, we attempted to simulate the propagation of a Gaussian using our FFT code. The results of this simulation are given in Figure 11.

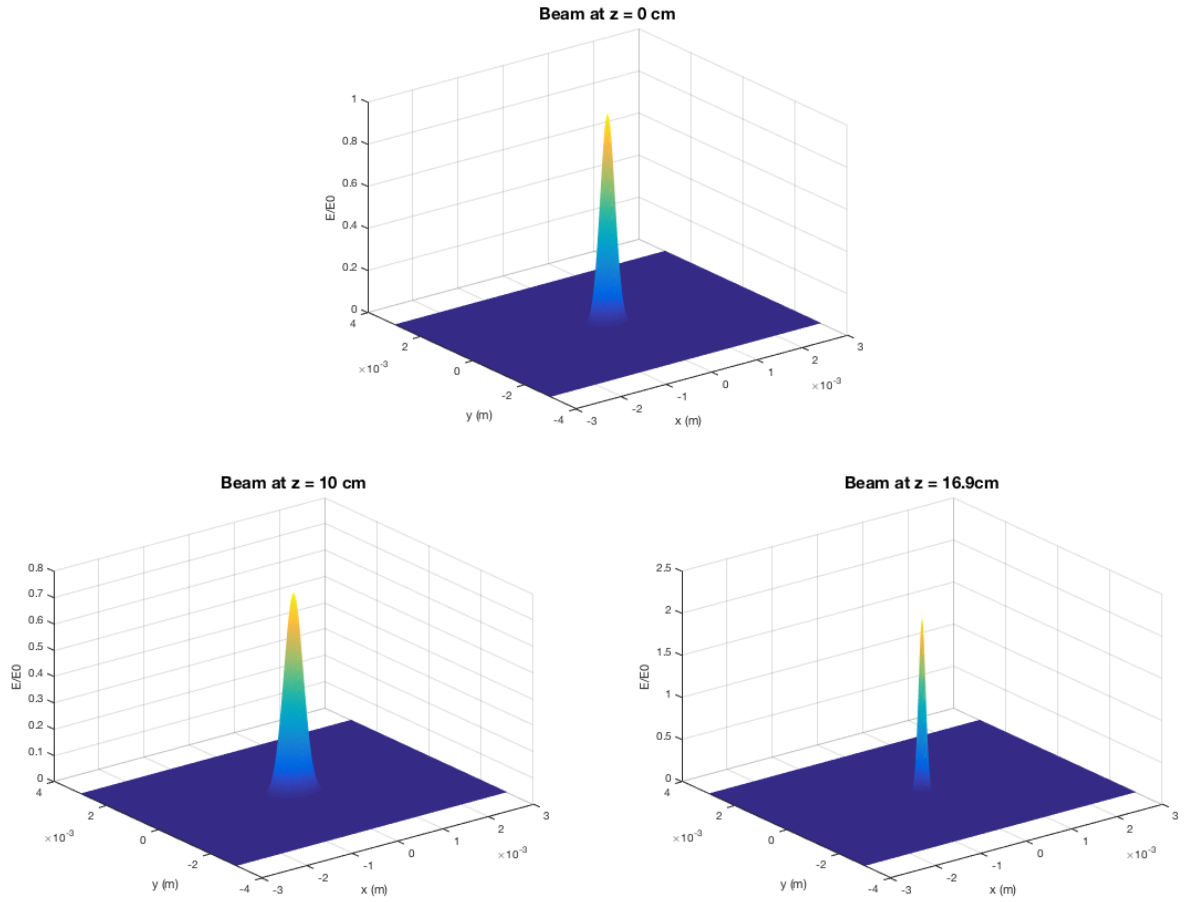

Figure 11: Mode shapes at z = 0cm, 10cm, 16.9cm

In order to determine the spot size of the beam, we plot the log of the field in one dimension direction against x^2 or y^2. For a Gaussian, this should be a linear with slope $-\frac{1}{w^2(z)}$.

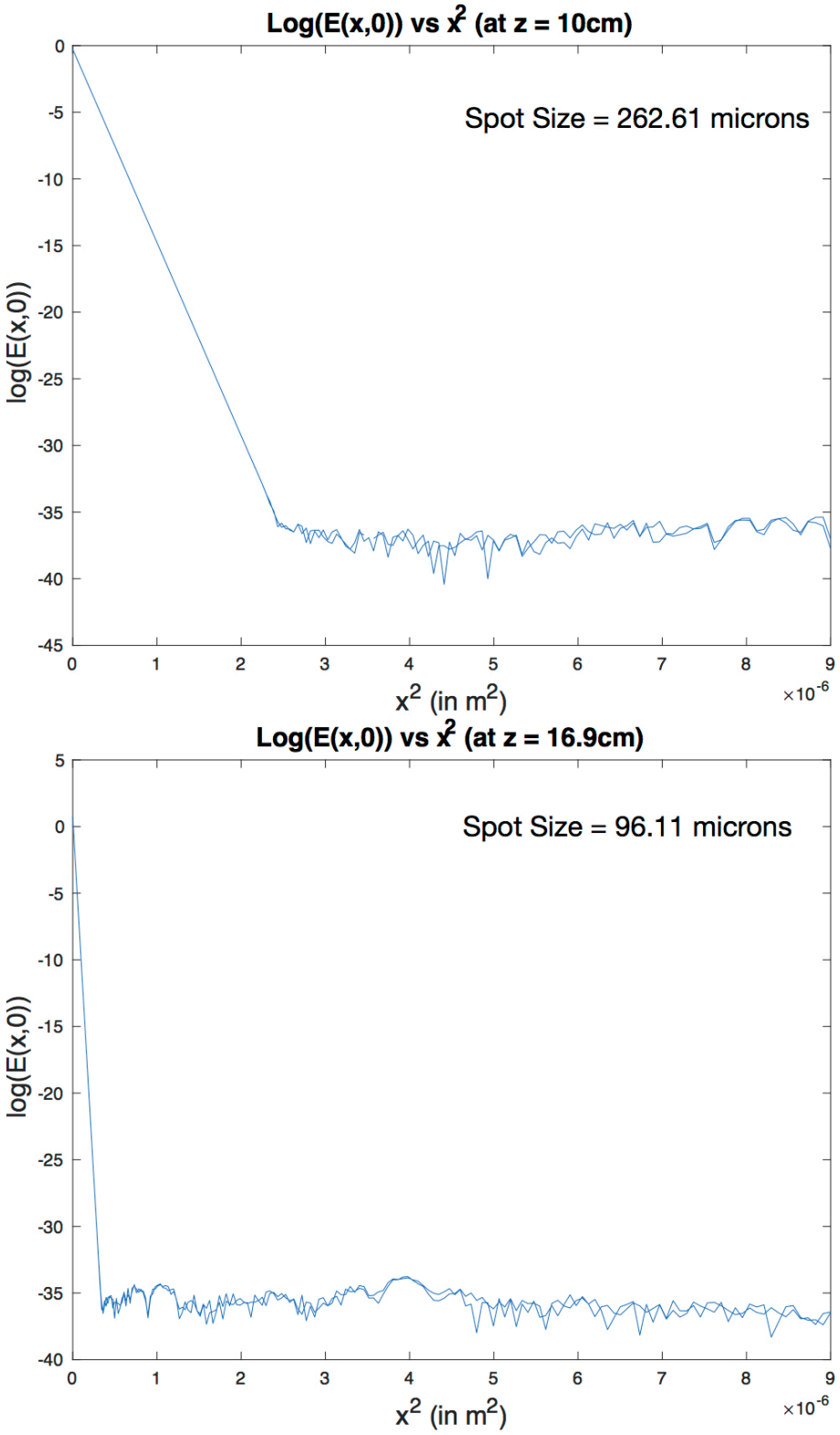

Figure 12: Log(E) plots for calculation of spot size

The graph becomes random and non linear(gaussian) after a point due to the round-off error while running the fft and ifft routines. That region is a tail of the distribution, far from the centre where values are neglibly small.

The values for the spot sizes obtained by FFT Propagation agree with those obtained using the ABCD matrices, which confirms that the FFT code is working properly.

2.5 To Do

2.5.1 Experimental Setup

- Profile both 1064nm and 532nm beams from the Innolight Diabolo using a Dataray beam profiler in order to find out where to set up the Faraday Isolators in front of the laser.
- Assemble the remaining components until the non-linear waveguide arrives.

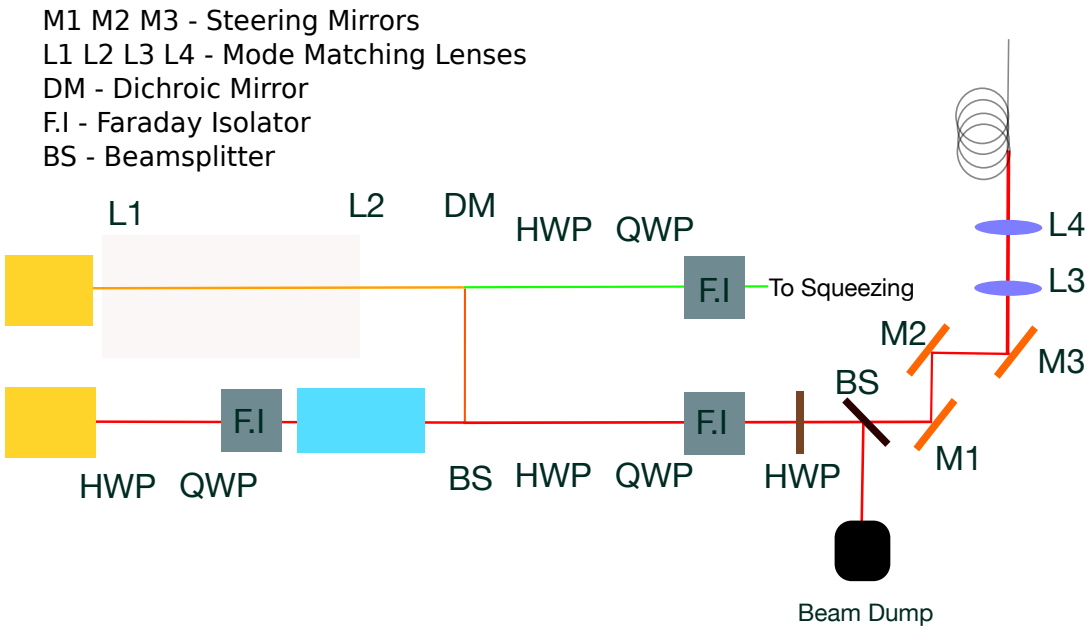

Figure 13: Laser Setup

2.5.2 FFT Propogation Code

Currently, the FFT propagation can only account for beams that do not change size very rapidly and stay well within the computation window for the FFT. Increasing the computation window decreases the resolution of sampling, while increasing the sampling resolution

drastically increases computation time. For the actual mode-matching, the code would have to have an adaptable computation window. We will implement an adaptable coordinate scaling method, which has been described by Hiro Yamamoto[11].

2.5.3 Waveguide Mode

Compare the mode obtain from the waveguide with a Gaussian and determine how to maximize the overlap, using free space propagation and mode matching lenses. The mode output by the waveguide, goes like $cos(ax)cos(by)$, within the boundaries of the waveguide and can be made equal to a Gaussian of approriate size to the second order.

2.5.4 Homodyne Detection

Design and assemble a transimpendance circuit for the photodetectors that will be used in the homodyning process.

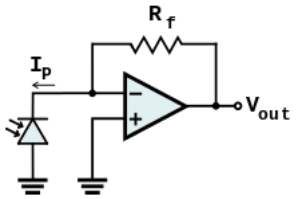

Figure 14: Simple Transimpedance Circuit

References

[1] LIGO Scientific Collaboration, *Advanced LIGO*. Class. Quant. Gravity 32, 074001 (2015)

[2] Buonanno, Alessandra and Chen, Yanbei, *Quantum noise in second generation, signal-recycled laser interferometric gravitational-wave detectors*

PhysRevD.64.042006

[3] LIGO Scientific Collaboration, *Instrument Science White Paper*. LIGO-T1600119v4 https://dcc.ligo.org/LIGO-T1600119/public

[4] LIGO Scientific Collaboration, *Enhanced sensitivity of the LIGO gravitational wave detector by using squeezed states of light* Nature Photonics 7, 613619 (2013)

[5] LIGO Scientific Collaboration, *A gravitational wave observatory operating beyond the quantum shot-noise limit* Nature Phys. 7, 962965 (2011)

[6] Alex Lvovsky, *Squeezed Light*. arXiv:1401.4118 .

[7] A. Ghatak and K. Thyagrajan , *Chapter 14, Optical Electronics*.

[8] Anthony Siegman, *Chapter 20, Lasers*.

[9] The Virgo Collaboration *Chapter 3, The VIRGO Physics Book Vol II - Optics and Related Topics.*

[10] M.S. Stefszky et al, *Balanced Homodyne Detection of Optical Quantum States at Audio-Band Frequencies and Below.*

[11] Hiro Yamamoto *Separation of adaptive scaling in the field propagation in x and y* LIGO-T1300995-v1